PAPER • OPEN ACCESS

Indoor Fast Neutron Generator for Biophysical and Electronic Applications

To cite this article: A Cannuli *et al* 2018 *J. Phys.: Conf. Ser.* **1014** 012001

View the article online for updates and enhancements.

IOP ebooks™

Bringing you innovative digital publishing with leading voices to create your essential collection of books in STEM research.

Start exploring the collection - download the first chapter of every title for free.

Indoor Fast Neutron Generator for Biophysical and Electronic Applications

A Cannuli[1,2], M T Caccamo[1,5], N Marchese[3,4], E A Tomarchio[6], C Pace[3,4] and S Magazù[1]

[1] Dipartimento di Scienze Matematiche e Informatiche, Scienze Fisiche e Scienze della Terra, Università di Messina, V.le F. Stagno D'Alcontres 31, 98166 Messina, Italia

[2] INFN - LNS - Istituto Nazionale di Fisica Nucleare - Laboratori Nazionali del Sud - Via Santa Sofia 62, 95123 Catania, Italia

[3] Dipartimento di Ingegneria Informatica, Modellistica, Elettronica e Sistemistica, Università della Calabria, Via P. Bucci, 87036 Arcavacata di Rende, Cosenza, Italia

[4] INFN – LNF - Istituto Nazionale di Fisica Nucleare - Laboratori Nazionali di Frascati - Via Enrico Fermi 40, 00044 Frascati, Roma, Italia

[5] INDAM, Istituto Nazionale di Alta Matematica "F. Severi", P.le Aldo Moro 5, 00185 - Roma, Italia

[6] Dipartimento Energia, Ingegneria dell'Informazione e Modelli Matematici, Università di Palermo, V.le delle Scienze, Ed. 9, 90128 Palermo, Italia
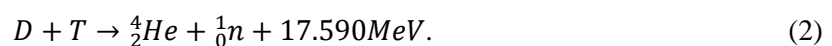
acannuli@unime.it

Abstract. This study focuses the attention on an indoor fast neutron generator for biophysical and electronic applications. More specifically, the findings obtained by several simulations with the MCNP Monte Carlo code, necessary for the realization of a shield for indoor measurements, are presented. Furthermore, an evaluation of the neutron spectrum modification caused by the shielding is reported. Fast neutron generators are a valid and interesting available source of neutrons, increasingly employed in a wide range of research fields, such as science and engineering. The employed portable pulsed neutron source is a MP320 Thermo Scientific neutron generator, able to generate 2.5 MeV neutrons with a neutron yield of 2.0 x 10^6 n/s, a pulse rate of 250 Hz to 20 KHz and a duty factor varying from 5% to 100%. The neutron generator, based on Deuterium-Deuterium nuclear fusion reactions, is employed in conjunction with a solid-state photon detector, made of n-type high-purity germanium (PINS-GMX by ORTEC) and it is mainly addressed to biophysical and electronic studies. The present study showed a proposal for the realization of a shield necessary for indoor applications for MP320 neutron generator, with a particular analysis of the transport of neutrons simulated with Monte Carlo code and described the two main lines of research in which the source will be used.

1. Introduction

For industrial applications that require neutrons, it is possible the employ of three different primary sources, such as nuclear reactors, radioisotopes and accelerator-based neutron sources. Nuclear reactors are clearly the largest and most prolific sources of neutrons, though their size, complexity and cost have limited their industrial applications for purposes other than electricity generation. In contrast, radioisotope neutron sources are employed in a myriad of industrial applications, including thickness gauging and petroleum exploration. Furthermore, radioisotope sources are ideal for fixed installations that run continuously, but they are not well suited for applications that require pulsed neutrons and they may create safety issues and logistical complications as well. Accelerator-based neutron sources are the third available source of neutrons for industrial applications. These systems vary in size and diversity and they include large installations, for example the spallation neutron source and the smaller photo-neutron sources. Among these accelerators, compact devices, known as fast Neutron Generators (NG)s are mostly employed in different fields that require neutrons. They are designed as hermetic, sealed tubes and use the following Deuterium–Deuterium (D–D) or Deuterium–Tritium (D–T) reactions:

$$D + D \rightarrow {}^{3}_{2}He + {}^{1}_{0}n + 3.270 MeV \qquad (1)$$

$$D + T \rightarrow {}^{4}_{2}He + {}^{1}_{0}n + 17.590 MeV. \qquad (2)$$

They are able to generate neutrons of an energy of 2.5 MeV in the case of D-D reactions and 14.1 MeV in the case of D-T reactions. In general, a fast NG is constituted by a source for generating positively charged ions; one or more devices to accelerate these ions; a metal hydride target loaded with either deuterium, tritium, or a mixture of the two and a gas-control reservoir, also made of the same material.

In this study the findings obtained by several simulations with MCNP Monte Carlo code, necessary for the realization of a shield for an indoor fast NG for biophysical and electronic applications, are presented. Furthermore, an evaluation of the neutron spectrum modification caused by the shielding is reported. The obtained results showed a proposal for the realization of a shield necessary for indoor applications for a MP320 NG, with a particular analysis of the transport of neutrons simulated with Monte Carlo code and described the two main lines of research in which the source will be used [1-10].

2. Fast Neutron Generator and shielding design calculations

Fast NGs are valid and interesting available sources of neutrons, increasingly employed in a wide range of research fields, such as science and engineering. The Thermo Scientific MP 320 is an example of very lightweight portable fast NG. It can be used in different applications like explosive, weapon detection, or drug detection and it can be employed in laboratories for different kind of research applications because it is a relatively compact system that requires a very low power. It is possible to operate with either a D-T or a D-D neutron tube, simply changing the target inside the neutron tube. In fact, in "D-T mode", the source is able to generate a neutron yield of 1.0×10^{8} n/s with an energy of 14.1 MeV, while in "D-D mode" it generates a neutron yield of 2.0×10^{6} n/s with an energy of 2.5 MeV. The NG can be modulated varying the pulse rate from 250 Hz to 20 kHz, varying respectively from 5% to 100% the duty factor. It can be also used in conjunction with an ORTEC PINS-GMX solid-state photon detector, made of n-type high-purity germanium. For indoor

application, such as research activities, the NG needs the realization of a specific bunker necessary to avoid damage from radiation exposition for users and instrumentation. Neutrons interact with nuclei in a variety of ways, for instance, if the nucleus is unchanged in either isotopic composition or internal energy after interacting with a neutron, the process is called elastic scattering. On the other hand, if the nucleus, still unchanged in composition, is left in an excited state, the process is called inelastic scattering. Generally, two or more neutrons are emitted when a nucleus is struck by a high energy neutron. There are three different procedures for the calculation of the shielding, which are neutrons transport equation, the Monte Carlo simulation and the removal cross section method.

Neutrons transport theory is relatively simple in principle and it is possible to determine an exact equation for transport phenomena, i.e. Boltzmann equation, also known as transport equation. Unfortunately, it is much easier to derive the Boltzmann equation than it is to solve it, though under some specific conditions, such as uniform materials and same energy for the neutrons, the equation simplifies considerably the problem and it can be calculated in a rather straightforward way. This simplified transport theory is known as neutron diffusion equation and it is shown in the following:

$$D \, \nabla^2 \phi - \Sigma_a \phi + s = \frac{1}{v} \frac{\partial \phi}{\partial t}. \tag{3}$$

However, many diffusion problems can not be solved by the analytical techniques; they have need of numerical computation methods [11].

Another different method shielding calculation is the Monte Carlo simulation. It consists of simulating individual particles and recording some aspects of their average behavior, using the central limit theorem. Monte Carlo simulation can be employed to duplicate theoretically a statistical process for complex problems that can not be modeled by computer codes, using deterministic methods. The individual probabilistic events of a process are simulated sequentially and the probability distributions, which govern the events, are statistically sampled to describe the total phenomenon.

Finally, the removal cross section method takes into account the ability of materials to remove neutrons of different energies from the primary beam. The interactions that slow neutrons down and cause their eventual removal from a beam are probabilistic, whereby a flux of neutrons of intensity I will be diminished in a thickness x of absorber proportionally to the intensity of the neutron source and the neutron removal coefficient Σ_{nr}, of the absorbing material:

$$-\frac{dI}{dx} = \Sigma_{nr} I. \tag{4}$$

The solution of the equation is:

$$I(x) = I_0 e^{-\Sigma_{nr} x} \tag{5}$$

in which, I_0 is the initial intensity, $I(x)$ refers to those neutrons that penetrate a distance x in the absorber without a collision, $e^{-\Sigma_{nr} x}$ is the probability that a given neutron travels at a distance x without any interaction. From a conceptual point of view, Σ_{nr} can be considered as the probability per unit path length that a neutron will undergo an interaction as it moves through an absorber and it will be removed from the beam by either absorption or scattering [11].

3. Experimental results for Thermo Scientific MP320 NG shielding
For the design of the MP320 NG shielding, the features in table 1 were taken as a reference.

Table 1. Features for the design of the MP320 NG shielding.

reaction	D-D
max neutron energy [MeV]	2.45
neutron yield [n s⁻¹]	2.00E+06

In order to perform a preliminarily evaluation of the shielding thicknesses was used the method of removal cross section. In a second moment, data preliminarily obtained were verified with MCNP Monte Carlo code simulations. The removal cross sections for different materials are available in several handbooks for shielding dimensioning, in particular, the employed materials for neutron shielding and their Σ_r are reported in table 2 [12-14].

Table 2. Materials employed for neutron shielding.

material	ρ [g cm⁻³]	Σ_r [cm⁻¹]
borated silicone (Elmahroug et al, 2013)	1.59	0.1007
30% borated PE (Elmahroug et al, 2013)	1.19	0.1191
iron (Kaye and Laby, 2005)	7.86	0.168
lead (Kaye and Laby, 2005)	11.35	0.116
barite concrete (NBS, 1957)	3.491	0.0945

In order to optimize the shielding size it is necessary to select materials that offer a good shielding power, i.e. an high Σ_r. It is also important to utilize the interactions of neutrons with the different materials in order to optimize the processes of slowing down and capture. Therefore the shielding is made of successive layers of different materials. The exponential attenuation law is valid only for collimated neutron beam, while in the case in which the source can be considered as a point source, the spatial dependence of the neutron flux has to be considered. Therefore the attenuation law becomes the following:

$$\acute{\Phi} = \frac{\varphi_0 e^{-\Sigma_r \cdot t}}{4\pi d^2} \tag{6}$$

where φ_0 is the initial neutron yield (n s⁻¹), d is the distance at which neutron flux is calculated respect to the source position, Φ is the neutron flux at distance d from the source and t is the thickness of shielding material. The method of removal cross section allows to obtain realistic estimations of the neutrons attenuation. Further evaluations can be performed using numerical codes based on the Monte Carlo method. The aim of the shielding is to reduce the neutron flux up to make the dose rate lower than the project limit. The evaluation of the different materials thickness was made considering their characteristics (Σ_r and weight). Therefore, the materials and thickness in table 3 were chosen.

**Table 3.** Materials and thickness for Neutron Generator MP320 shielding.

material	Σ_r [cm⁻¹]	t [cm]
30% borated PE	0.1191	15
barite concrete	0.0945	15

Neutron flux was calculated on the external surfaces at the end of the shielding, taking in consideration the distance between the source, considered a point source, the internal surface of the shielding and the entire shielding thickness. The values of neutron flux obtained for the different surfaces are shown in table 4.

Table 4. Neutron flux values obtained for the different surfaces of the shielding.

	shielding							
	up		**lateral**		**back**		**front**	
material	t [cm]	$\acute{\phi}$ [n cm^{-2} s^{-1}]	t [cm]	$\acute{\phi}$ [n cm^{-2} s^{-1}]	t [cm]	$\acute{\phi}$ [n cm^{-2} s^{-1}]	t [cm]	$\acute{\phi}$ [n cm^{-2} s^{-1}]
air	33	146.15	15	397.89	23	300.86	57	48.99
30% borated PE	15	11.57	15	21.77	15	18.47	30	0.59
barite concrete	15	1.63	15	2.59	15	2.30	0	0.59

In figure 1, it is possible to see the different thicknesses of the shielding: the green part represents the 30% borated PE, while the grey part, barite concrete.

Figure 1. Representation of shielding thicknesses (a), shielding section view (b) and shielding structure (c).
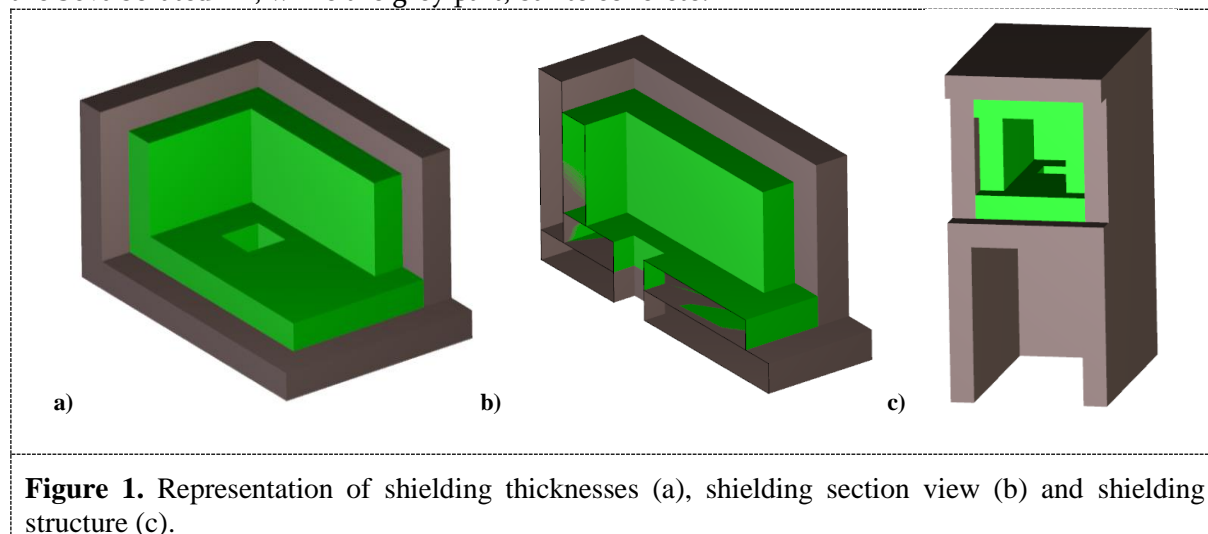
In the section view, it is possible to identify the window for the samples irradiation. NG will be located inside the shielding, with the neutron emitting target in correspondence of the window. The entire shielding will be sustained by a concrete structure as shows in figure 1 (c). Figure 2 shows the shielding inside the laboratory and the comparison between the shielding and a user.
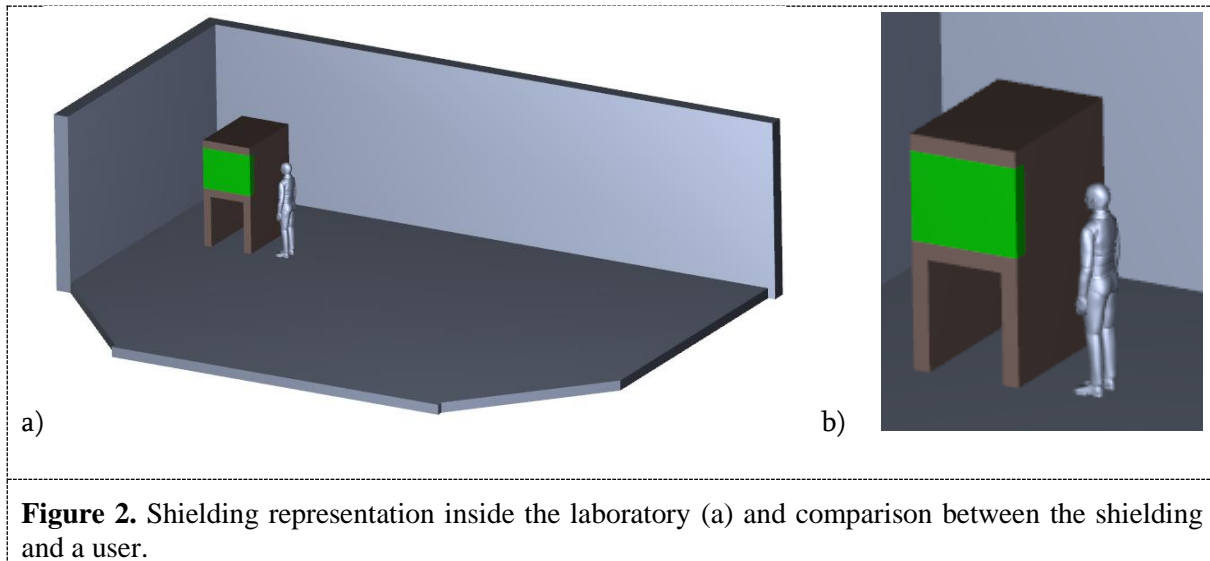
Figure 2. Shielding representation inside the laboratory (a) and comparison between the shielding and a user.

Several simulations were performed with a software based on Monte Carlo method, in order to verify the values obtained with the application of removal cross section. The code used was MCNP5. The code include information relatively to the geometry, materials and source characteristics. The cells in which evaluate the neutron flux were also specified. These were placed on the external surfaces of the shielding in correspondence of the specification addressed in the design phase. For neutron flux evaluation was chosen the Track Length Estimate of Cell Flux (F4) that allow to obtain the average neutron flux in a volume V, as described in following formulation:

$$\overline{\phi_V} = \frac{1}{V} \int dE \int dV \int ds \, N(\vec{r}, E, t) \tag{7}$$

where $N(\vec{r}, E, t)$ is the density of particles, regardless of their trajectories, at a point.

Thus, the code studies the life of the particles generated into the source and then evaluates their average behavior in the volume V. Therefore, taking into consideration the complexity of the problem, it will be necessary to simulate an adequate number of particles in order to reduce the uncertainty on the flux values.

Two sections of the shielding are reported in figure 3: the blue part represents 30% Borate PE, the yellow part, barite concrete and the green part, the cells in which neutron flux was calculated. The cross in the two figures shows the point at which the "neutron source" is located.
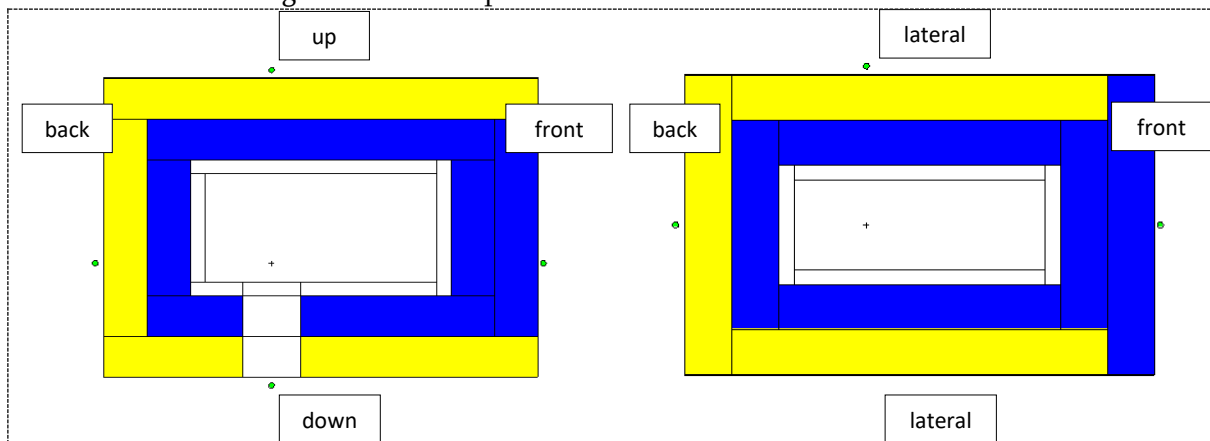
Figure 3. Shielding sections from MCNP simulations.

Simulations were performed considering the life of $2 \cdot 10^9$ neutrons, in order to evaluate the flux in the green cells and in order to obtain a standard deviation under the 10%. The values obtained by the simulation represent the average flux into the cells volume for every neutron started from the source.

They must be handled in order to obtain the value of the mean flow in the cells. After handling the values, the results in table 5 were obtained.

Table 5. Neutron flux values obtained by Monte Carlo simulation.

	shielding			
	up	**lateral**	**back**	**front**
energy [MeV]	$\acute{\Phi}$ **[n cm⁻² s⁻¹]**	$\acute{\Phi}$ **[n cm⁻² s⁻¹]**	$\acute{\Phi}$ **[n cm⁻² s⁻¹]**	$\acute{\Phi}$ **[n cm⁻² s⁻¹]**
2.45	0.349	0.103	0.252	8.87×10^{-3}
total	3.75	1.61	2.63	0.145

Comparing the values obtained from the simulation with those obtained by the removal cross section method, as shown in table 6, it is possible to verify that this method allows to obtain the realistic values of the neutron flux and it represents a valid approach to determine neutron shielding thicknesses.

Table 6. Comparison between Removal Cross Section Method and Monte Carlo Method.

	shielding			
	up	**lateral**	**back**	**front**
	$\acute{\Phi}$ **[n cm⁻² s⁻¹]**	$\acute{\Phi}$ **[n cm⁻² s⁻¹]**	$\acute{\Phi}$ **[n cm⁻² s⁻¹]**	$\acute{\Phi}$ **[n cm⁻² s⁻¹]**
Σ_r **method**	1.63	2.59	2.30	0.59
MCNP total	3.75	1.61	2.63	0.145

In order to evaluate the effect of shielding, it is possible to calculate the neutron dose rate. The following parameters were taken into account as references for the dose rate limits evaluation:
· Project Equivalent Dose [mSv/y]   0.5;
· Annual duty hours [h/y]   1.200.

The project neutron dose rate was chosen as half of the annual limit for the population in order to consider also the photons contribute to the total dose rate. The annual duty hours were chosen as the typical lifetime of the target. Taking into account of the set parameters, the reference value for the dose rate is equal to:

$$\frac{0.5 \left[\frac{mSv}{y}\right]}{1,200 \left[\frac{h}{y}\right]} = 4.2 \cdot 10^{-4} \left[\frac{mSv}{h}\right]. \tag{8}$$

In order to evaluate the neutron dose rate, it is necessary to know the neutron spectrum and to apply the flow-to-dose rate energy-dependent conversion factors. Considering the neutron spectrum obtained with MCNP simulations and applying the conversion factors, the dose rate values, shown in table 7, were obtained [15-16].

**Table 7.** Equivalent Dose Rate values outside the neutron shielding.

	shielding			
	up	**lateral**	**back**	**front**
equivalent dose rate [mSv/h]	1.51×10^{-3}	2.81×10^{-2}	$4.0E \times 10^{-2}$	1.62×10^{-2}
equivalent dose rate @ 0.1 m from the shielding [mSv/h]	1.20×10^{-8}	2.23×10^{-7}	3.18×10^{-7}	1.29×10^{-7}

The obtained values of neutron dose rate are over the limit of $4.2 \cdot 10^{-4} [mSv/h]$, however, taking into account the geometric attenuation is possible to evaluate that the neutron dose rate goes down rapidly below the limit.

Every application field of neutron sources needs particular characteristics of irradiation and it is necessary to evaluate if the source is suitable for the tests. The shielding or other structural materials cause the modification of the energy spectrum of a neutron source and, hence, of the exposed samples. Therefore it is necessary to evaluate the modified energy spectrum in order to define the real characteristics of the neutron source. Several simulations were performed to this aim, using MCNP. The neutron spectrum was evaluated in correspondence to the window for the irradiation of the samples, outside the shielding, as shown in figure 4.
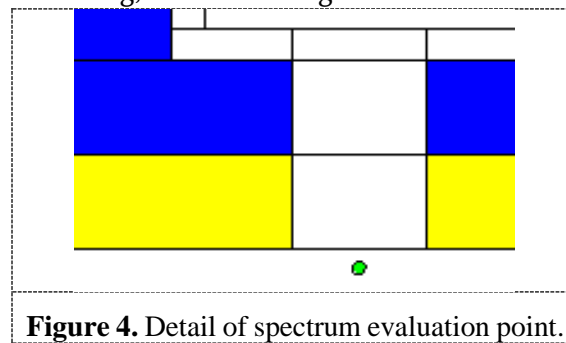
Figure 4. Detail of spectrum evaluation point.

The simulations were performed both for the D-D and D-T mode in order to evaluate the effect of shielding on the two different energy neutron beams.

Figure 5. a) D-D neutron spectrum; b) D-T neutron spectrum.
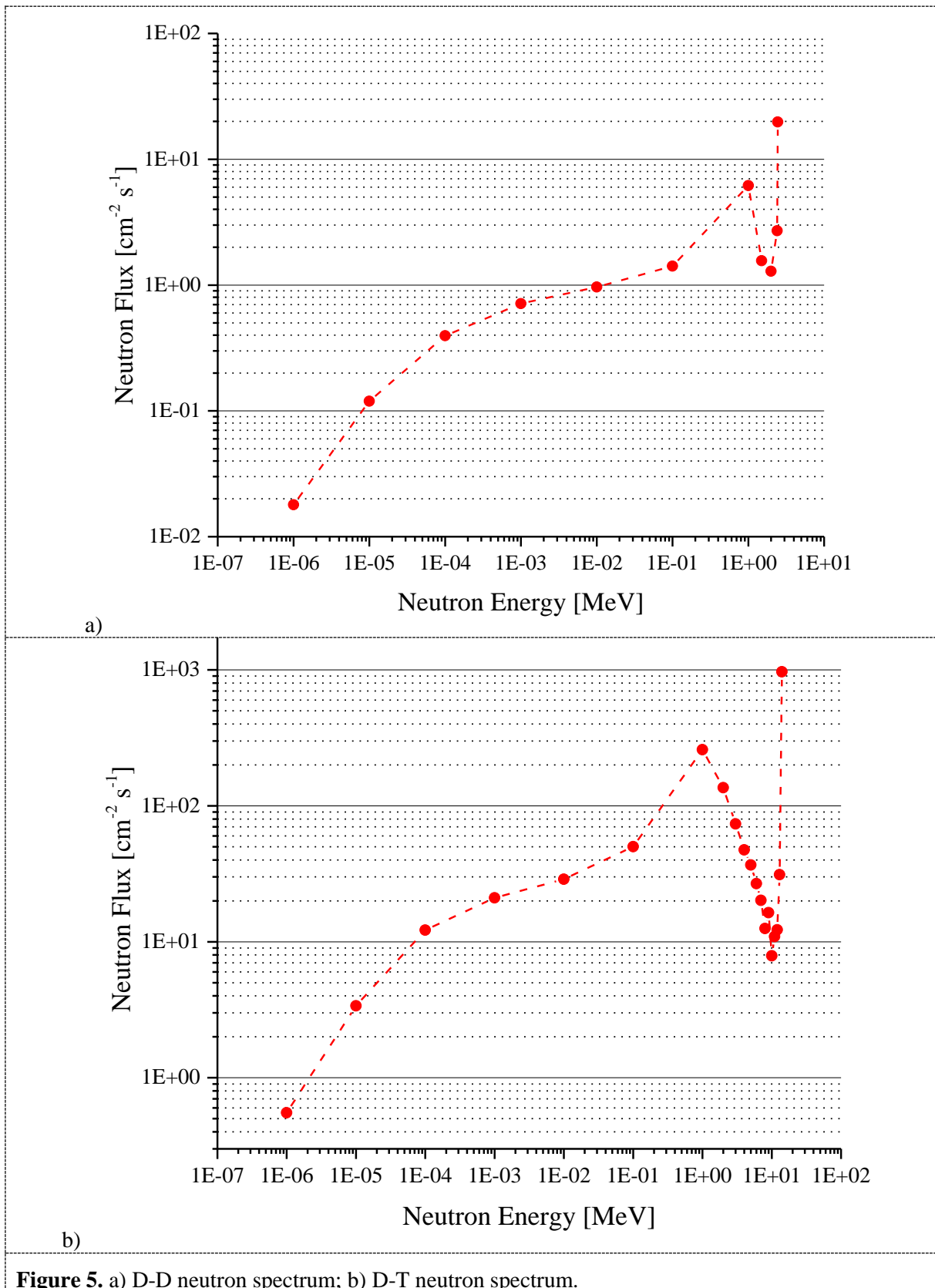
The graphics in figure 5 show how the presence of the shielding contributes to the spectrum change to which the samples will be exposed.

4. Biophysical and electronic applications

The indoor MP320 NG can be employed both for biophysical and electronic applications, some example are elemental analysis and testing of devices. Elemental analysis, known as Neutron Activation Analysis (NAA) is an analytical technique for qualitative and quantitative multi-elemental analysis of major, minor and trace elements. For example, with this technique, it is possible to trace heavy metals in samples of biophysical interest that contain aqueous solutions [17-21], disaccharides [22-39] or polymers [40-47] and which have already been studied with other spectroscopic techniques [48-51]. In NAA, a target, after a non-elastic collision in the atomic nucleus, absorbs a neutron and forms a compound in an excited state. When the compound nucleus de-excites into a more stable configuration, an emission of one or more characteristic prompt gamma rays occurs. The process ends when the ground state formed during the de-excitation, is stable, i.e. at the moment in which an isotope of the same element, with a mass number increased by one, is produced. Generally, every chemical element has at least one isotope that produces a radioactive one in neutron capture. They typically emit β particles and γ radiation with a given half-life. The energies of the prompt and delayed gamma rays allow to identify the emitter nuclide and their intensity is proportional to its amount.

The Earth's atmosphere acts as a shield against ionizing radiation coming from deep space. However, the interaction of galactic cosmic rays with the terrestrial atmosphere produces a "shower" of secondary particles, mainly neutrons, which come down to sea level [52]. Thus, all electronic devices are exposed to this "natural" radiation environment. Despite the neutron flux is quite low (especially at sea level) even a single neutron, under certain conditions, can cause a failure into electronic devices: this case is known as Single Event Effects (SEE)s [53]. SEEs are related to the charge generated in the semiconductor, through ionization realized by the incident particle. In the case of neutrons, this mechanism is activated by the emission of secondary charged particles, after a nuclear reaction, radioactive decay or spallation [54]. If the ionization takes place near a reverse biased pn junction, the electron-hole pairs are separated by the electric field and then collected by the electrodes, generating a transient current. This microscopic mechanism can lead to different macroscopic effects, as for example, Single Event Upset (SEU) in a memory [55] or Single Event Burnout (SEB) affecting power MOSFETs [56]. In order to characterize a device's sensitivity to terrestrial neutrons, it is necessary to perform accelerated tests with dedicated neutron facilities. The procedures to carry out such tests and the required featured of the facilities are regulated by international standards such as the JESD89A. The scope of these tests is to assess the failure rate associated with terrestrial neutron SEE.

Spallation and mono-energetic sources are suggested for testing devices with high-energy neutrons. Spallation sources produce a "white" neutron spectrum, which mimics the natural terrestrial neutron environment. A valid alternative could be represented by mono-energetic facilities. There are only few mono-energetic neutron sources: D-T and D-D facilities, respectively at 14 MeV and 2.45 MeV. According with the standard JESD89A. In this context, the proposed neutron facility could be used for accelerated *SEE* testing of electronic devices.

Conclusions

The data obtained with the method of removal cross section and through simulations with MCNP represent a fundamental aid in the design of the shield, necessary for the indoor use of the neutron source. This work is therefore a starting point for the construction of the shield and the obtained data will be verified experimentally. The project could be subjected to modifications in order to optimize the irradiation characteristics of the samples. The employed predictive tools will be so critical to the optimization process and will allow to intervene on the shielding before its construction. The whole device represent a valid research tool and the areas where it can be used are numerous and biophysics and electronics represent only two examples of the many possible uses of this facility. The reduced operating costs, the compactness and the possibility of varying the duty factor make the neutron generator a very competitive device within the panorama of the available neutron sources.

References

[1]   Csikai J 1987 *CRC Handbook of Fast Neutron Generators* (Boca Raton: CRC Press)

[2]   James W D 2000 *J. Radioanal. Nucl. Chem.* **243** 119

[3]   Marchese N, Cannuli A, Caccamo M T and Pace C 2016 *Biochim. Biophys. Acta* **1861** 3661-3670

[4]   Chichester D L and Simpson J D 2003-2004 *The Industrial Physicist, American Institute of Physics* **9** 22

[5]   Reijonen J 2005 Compact Neutron Generators for Medical, Home Land Security and Planetary Exploration, *Proceedings of the IEEE* 49-53

[6]   Ludewigt B A, Wells R P and Reijonen J 2007 *Nucl. Instrum. Methods Phys. Res. B* **261** 830-834

[7]   Das B K and Shyam A 2008 *Rev. Sci. Instrum.* **79** 123305

[8]   Hennet L *et al.* 2011 *Eur. Phys. J. Spec. Top.* **196** 151-165

[9]   Liang L, Rinaldi R and Schober H 2009 *Neutron Applications in Earth, Energy and Environmental Sciences* (New York: Springer)

[10] Liu W, Li M, Gao K and Gu D 2014 *Nucl. Instrum. Methods Phys. Res. A* **768** 120–123

[11] Lamarsh J R 1966 Introduction to Nuclear Reactor Theory. *Addison-Wesley Publishing Company* 17-118-132-152

[12] National Bureau of Standards 1957 *Protection against neutron radiation up to 30 Million electron Volts* **63** 81

[13] Kaye G W C and Laby T H 1995 *Tables of Physical & Chemical Constants Kaye & Laby Online*

[14] Elmahroug Y, Tellili B and Souga C. 2013 *Intern. J. Phys. Res.* **3** 11

[15] Seog-Guen K *et al.* 1980 *J. Korean Phys. Soc.* **12** 173

[16] Ward D C 2009 Impact of switching to the ICRP-74 neutron flux-to-dose equivalent rate conversion factors at the sandia national laboratory building 818 neutron source range 1144

[17] Lokotosh T V, Magazù S, Maisano G and Malomuzh N P 2000 *Phy.s Rev. E – Stat. Physics, Plasmas, Fluids, Relat. Interdiscip.* **62** 3572-3580

[18] Magazù S 1996 *Phys. B.* **226** 92-106

[19] Magazù S, Maisano G, Mallamace F and Micali N 1989 *Phys. Rev. A* **39** 4195-4200

[20] Jannelli M P, Magazù S, Migliardo P, Aliotta F and Tettamanti E 1996 *J. Phys. Condens. Matter.* **8** 8157-8171

[21] Magazù S, Migliardo F and Telling M T F 2008 *Food Chem.* **106** 1460-1466

[22] Magazù S, Calabrò E, Caccamo M T and Cannuli A 2016 *Curr. Chem. Biol.* **10** 57-64

[23] Magazù S, Maisano G, Migliardo P, Middendorf H D and Villari V 1998 *J Chem Phys.* **109** 1170-1174

[24] Magazu S *et al.* 1998 *J. Phys. Chem. B* **102** 2060-2063

[25] Pagnotta S E, Ricci M A, Bruni F, McLain S and Magazù S 2008 *Chem. Phys.* **345** 159-163

[26] Magazù S, Migliardo F and Telling M T F 2007 *Eur Biophys J.* **36** 163-171

[27] Minutoli L *et al.* 2007 *Shock* **27** 91-96

[28] Magazù S, Calabrò E and Campo S 2010 *J. Phys. Chem. B* **114** 12144-12149

[29] Barreca D *et al.* 2010 *Biophys. Chem.* **147** 146-152
[30] Migliardo F, Caccamo MT and Magazù S 2014 *Food Biophys.* **9**
[31] Magazù S, Migliardo F, Vertessy B G and Caccamo M T. 2013 *Chem Phys.* 424
[32] Migliardo F, Caccamo M T and Magazù S 2013 *J. Non Cryst. Solids.* 378
[33] Magazù S, Migliardo F, Vertessy B G and Caccamo M T 2013 *Chem. Phys.* **424** 56-61
[34] Branca C, Magazù S, Maisano G, Bennington A and Fåk B 2003 *J. Phys. Chem. B* **107** 1444-1451
[35] Barreca D, Lagana G, Bruno G, Magazù S and Bellocco E 2013 *Biochim.* **95** 2042-2049
[36] Branca C, Magazù S, Migliardo F and Migliardo P 2002 *Phys. A* **304** 314-318
[37] Branca C *et al.* 1999 *J. Phys Cond. Matter.* **11** 3823-3832
[38] Magazù S *et al.* 2013 Nova Science Pub. 35-46
[39] Branca C *et al.* 1999 *J. Phys. Cond. Mat.* **11** 3823-3832
[40] Caccamo M T, Cannuli A, Calabrò E and Magazù S 2017 *IOP Conf. Ser. Mater. Sci. Eng.* **199** 12119
[41] Faraone A, Magazù S, Maisano G, Ponterio R and Villari V 1999 *Macromol.* **32** 1128-1133
[42] Branca C, Magazù S, Maisano G, Migliardo P and Villari V 1998 *J. Phys. Condens. Matter.* **10** 10141-10157
[43] Migliardo F, Magazù S and Caccamo M T 2013 *J. Mol. Struct.* **1048** 261-266
[44] Caccamo M T and Magazù S 2016 *Vib. Spectrosc.* **85** 222-227
[45] Caccamo M T and Magazù S 2017 *Appl. Spectrosc.* **71** 401-409
[46] Caccamo M T and Magazù S 2017 *Spectrosc. Lett.* **50** 130-136
[47] Caccamo M T and Magazù S 2017 *Polym. Testing* **62** 311-318
[48] Magazù S, Migliardo F and Caccamo M T 2013 *Adv. Mater. Sci. Eng.* 1-7
[49] Caccamo M T and Magazù S 2017 *Eur. J. Phys.* **38**
[50] Caccamo M T, Calabrò E, Cannuli A and Magazù S 2016 *MATEC Web Conf.* **55** 02004
[51] Magazù S, Migliardo F and Caccamo M T 2012 *J. Phys. Chem. B* **116** 9417-9423
[52] Ziegler J F 1998 *IBM J. Res. Develop.* **42** 117-140
[53] Leray J L 2007 *Microelec. Rel.* **47** 1827-1835
[54] Tang H H K 1996 *IBM J. Res. Develop.* **40** 91-108
[55] Hands A, Morris P, Dyer C, Ryden K, and Truscott P 2011 *IEEE Trans. Nucl. Sci.* **58** 2687-2694
[56] Oberg D L, Wert J L, Normand E and Wender S A 1996 *IEEE Trans. Nucl. Sci.* **43** 2913-2920